JOURNAL OF MATERIALS SCIENCE 14 (1979) 70–85

The influence of hydrogen in the nitriding gas on the strength, structure and composition of reaction-sintered silicon nitride

M. W. LINDLEY, D. P. ELIAS, B. F. JONES, K. C. PITMAN
Admiralty Marine Technology Establishment, Holton Heath, Poole, Dorset, UK

The influence of hydrogen in a "static" and "flowing" nitriding gas on the mechanism of formation, composition, structure and mechanical properties of reaction-sintered silicon nitride has been investigated. Using previously developed structural and compositional models describing the progressive formation of silicon nitride, it is suggested that hydrogen enables a high partial pressure of silicon monoxide to be maintained at the early stages of nitridation, thus promoting the rapid development of a continuous skeletal network of silicon nitride with resultant high strength. The mechanisms of formation, composition, structure and mechanical properties of silicon nitride formed from one type of silicon compact under a variety of nitriding conditions are compared, and the significance of the nitriding atmosphere in determining properties is demonstrated.

1. Introduction

It has been appreciated for many years (for example [1]) that ceramics based on silicon nitride have properties that could be exploited in high-temperature engineering applications such as gas turbines. Considerable advances have been made towards this objective and gas turbines for vehicular use (for example [2]) and for electric power generation (for example [3]) are being evolved using these and related materials: more recently the use of silicon nitride in diesel engines has been considered [4]. For some of these applications reaction-sintered silicon nitride is a prime candidate for certain component parts but, to design effectively with this brittle material, it is essential that it be fabricated with consistent properties that are reproducible from batch to batch of material (for example [5]).

Some of the processing factors influencing strength variability have been reported (for example [6–9]). In particular gas flow during nitriding has been shown to degrade strength and it has been suggested [7] that undetected leaks in nominally "static" nitriding systems could produce sufficient gas flow to adversely affect strength.

Recently we have demonstrated [10] that the use of flowing nitrogen/hydrogen gas mixtures eliminates the adverse effect of gas flow on strength when nitrogen alone is used, and that the strengths of compacts reacted in "static" nitrogen, "static" nitrogen/hydrogen gas mixtures or "flowing" nitrogen/hydrogen gas mixtures are not significantly different. It has been reported [11] that the addition of hydrogen to a "static" nitriding gas can improve the strength and creep properties of reaction-sintered silicon nitride, although we have not confirmed [10] any significant strength improvements using "static" conditions in our particular experimental system.

The precise influence of hydrogen in the nitriding gas on the mechanism of formation, composition and strength of reaction-sintered silicon nitride is not well understood, and this paper addresses the problem. Experiments have been performed where silicon compacts have been reacted to differing degrees of conversion under "static" and "flowing" conditions in a 95% nitrogen/5% hydrogen gas mixture. The critical defect sizes ($2a$) of these materials have been calculated from measured values of strengths, elastic constants and critical stress intensity factors (K_{IC}); the proportions of α- and β-silicon nitride in the strength bars have been determined and their fracture surfaces examined. These data have

TABLE I Nitrided density, weight gain and strength data for bars nitrided in 95 N_2 / 5 H_2. Series (a) experiments

Experiment		Static/flow (Flow rate 100 ml min^{-1})*	Strength bars		
Time (h)	Temperature (° C)		Weight gain (%)	Nitrided density ($Mg\,m^{-3}$)	Mean strength ($MN\,m^{-2}$)
0†	1100	Static	0.5 ± 0.2	1.62	19 ± 1
0†	1175	Static	6.4 ± 1.1	1.71	43 ± 9
0†	1200	Static	13.1 ± 1.3	1.83	88 ± 8
5	1220	Static	36.5 ± 0.6	2.17	139 ± 9
5	1300	Static	47.0 ± 0.5	2.37	172 ± 16
20	1300	Static	49.8 ± 0.6	2.40	193 ± 9
20	1330	Static	51.9 ± 0.8	2.45	206 ± 26
0†	1100	Flow	0.3 ± 0.1	1.62	17 ± 2
0†	1200	Flow	5.8 ± 1.5	1.71	43 ± 8
0†	1150	Flow	7.4 ± 1.6	1.71	54 ± 9
0†	1190	Flow	13.2 ± 1.6	1.82	84 ± 9
1	1200	Flow	17.1 ± 1.2	1.89	91 ± 7
5	1200	Flow	20.5 ± 0.8	1.95	105 ± 6
5	1300	Flow	35.9 ± 2.2	2.20	140 ± 7
5	1330	Flow	42.0 ± 1.8	2.28	162 ± 9
20	1330	Flow	53.5 ± 1.1	2.48	216 ± 8

*Linear flow rate 25 mm min^{-1} past the samples.
†Furnace-cooled immediately reaction temperature achieved.

been compared with data for samples reacted in 100% nitrogen and interpreted in terms of previously elucidated compositional [8, 9] and structural models [12, 13] describing the formation of reaction-sintered silicon nitride: the role of hydrogen in the nitriding gas is then discussed.

Finally the mechanisms of formation, composition, microstructure and fracture properties of one type of silicon compact reaction-sintered under differing well-defined nitriding conditions are compared and related to our two models in an attempt to provide a basic framework against which experimental observations can be assessed.

2. Experimental

The silicon powder (median particle size 13 μm) was from the same powder batch previously described [12]. From this work it was known that the strength of silicon nitride bars prepared from this powder by our nitriding techniques are controlled by surface breaking inter-network pores of the bulk microstructure rather than some special defect (for example machining damage, impurity particles, etc. [12]). This powder was isostatically pressed at 185 $MN\,m^{-2}$ and argon-sintered for 4 h at 1175° C to produce a silicon compact with a green density of 1.60 $Mg\,m^{-3}$ from which strength bars, modulus bars and double torsion K_{IC} plates were cut [12]. The double torsion plates were notched and grooved in the green state. Nitriding experiments were in the temperature range 1100 to 1330° C (heating rate 50° C h^{-1}) under "static" or gas "flow" conditions [7] (flow rate 100 ml min^{-1})* using a 95% N_2/5% H_2 gas mixture (by volume)† at a total pressure of 1.1 bar: these experiments are designated series (a). The furnace contents and positions of the samples within the furnace were identical from experiment to experiment and consisted of six strength bars, two modulus bars and two double torsion plates. Green and nitrided densities, strengths, elastic moduli, K_{IC} and the weight percentages of the α-Si_3N_4, β-Si_3N_4 and silicon phases were determined by methods that have been described elsewhere [8, 12]. The fracture surfaces of strength bars were characterized by stereo-optical and by scanning electron microscopy: in particular the existence or absence of fracture origins and fracture mirrors was noted for each strength bar. Isothermal reaction rate data were also obtained for these compacts reacted in "static" and "flowing"* nitrogen and 95 N_2/5 H_2.

In another experimental series [series (b)] strength bars (green density 1.60 $Mg\,m^{-3}$) prepared by the same techniques from the same silicon powder batch were nitrided under "static" and

*A linear flow rate of 25 mm min^{-1} past the samples.
†Gas concentrations expressed as volume percentages.

"flow" conditions in nitrogen, or gas mixtures by volume of 99 $N_2/1$ H_2, 98 $N_2/2$ H_2, 95 $N_2/5$ H_2 and 90 $N_2/10$ H_2 for 5 h at 1300° C: gas flow rates were either 100 ml min^{-1} or 500 ml min^{-1}. The nitrided density and strengths [10] nitrogen weight gains and phase composition of these bars were determined.

3. Results

3.1. Mechanical properties

Table I shows nitriding temperatures and times for series (a) experiments together with the weight gains and nitrided densities of the bars and their fracture strengths. The experimentally determined Young's moduli (E), Poisson's ratios (ν) and strengths are plotted against the nitrided density (ρ_n) in Figs. 1 to 3: since "static" and "flow" data cannot be separated, these data have been considered as a single group "static plus flow". Straight lines were fitted to the grouped "static plus flow" data for E, σ and G (rigidity modulus) for all densities, and also to the grouped "static plus flow" data for nitrided densities greater than 1.8 Mg m^{-3} (equivalent to about 18% conversion of the silicon compact) with "faired-in" curves extending these lines to lower densities. These latter representations (see Section 4.2) are subsequently referred to as "best fit lines" and are now used in preference to the previous linear representations which include all values of ρ_n. The equations for the linear parts of these best fit lines and the equivalent data for identical compacts reacted in 100 N_2 [12] are listed in Table II, together with the grouped "static plus flow" strength data for series (b) experiments. The series (a) and (b) strength data are not significantly different from the equivalent data for silicon compacts reacted in "static" nitrogen [12]: the data from all three groups of experiments however

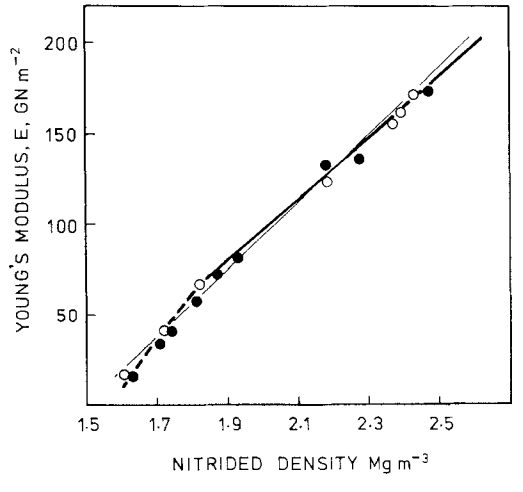

Figure 1 Young's modulus versus nitrided density (ρ_n) for silicon compacts nitrided in "static" and "flowing" 95 $N_2/5$ H_2 series (a). [– – – "best fit" line "static plus flow" (linear for $\rho_n > 1.8$ Mg m^{-3}). ——— linear relationship for all ρ_n "static plus flow". ○ "static" points. • "flow" points].

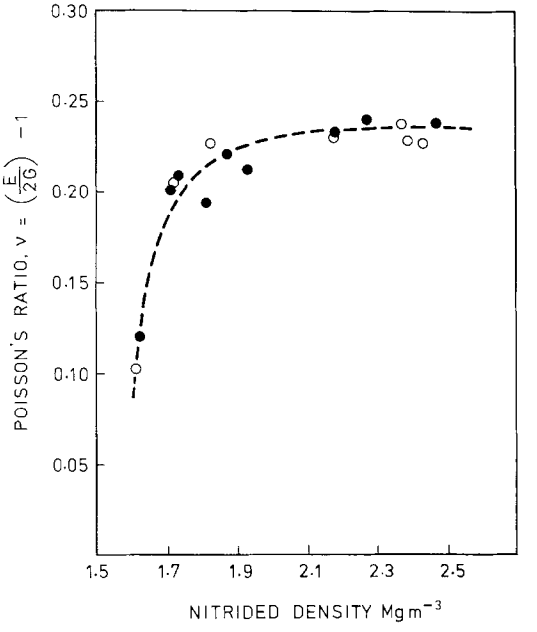

Figure 2 Poisson's ratio versus nitrided density for silicon compacts nitrided in "static" and "flowing" 95 $N_2/5$ H_2, series (a). Symbols as in Fig. 1.

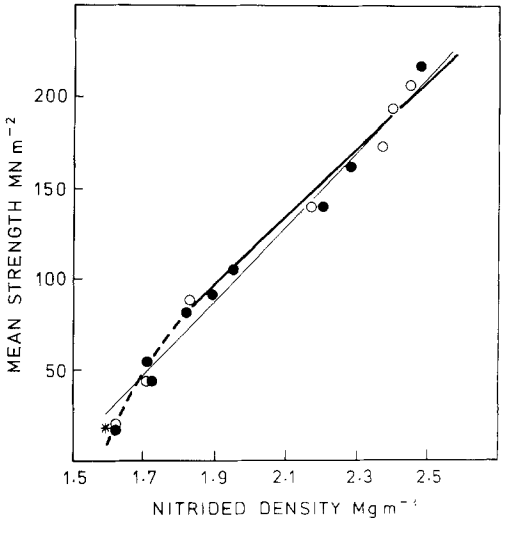

Figure 3 Mean strength versus nitrided density for silicon compacts nitrided in "static" and "flowing" 95 $N_2/5$ H_2, series (a). Symbols as in Fig. 1. (*Un-nitrided silicon compact).

TABLE II Linear equations of strength (σ), Young's modulus (E) and rigidity modulus (G) versus density (ρ_n) for various nitriding conditions

Nitriding	Density range	Equation	Correlation coefficient
Series (a) 95 N_2/5 H_2. Grouped "static" and "flow" data	All values ρ_n	$\sigma = 208\rho_n - 307$	0.988
		$E = 184\rho_n - 276$	0.997
		$G = 74\rho_n - 111$	0.997
	"Best fit lines" $\rho_n > 1.8$ Mg m^{-3}	$\sigma = 189\rho_n - 264$	0.987
		$E = 173\rho_n - 250$	0.997
		$G = 70\rho_n - 103$	0.996
Series (b). Grouped "static" and "flow" data [10]	"Best fit line" $\rho_n > 1.8$ Mg m^{-3}	$\sigma = 192\rho_n - 270$	0.988
100 N_2 * (static)	"Best fit lines" $\rho_n > 1.8$ Mg m^{-3}	$\sigma = 189\rho_n - 257$	0.997
		$E = 171\rho_n - 251$	0.999
		$G = 68\rho_n - 98$	0.999
100 N_2 * (flow)	All values ρ_n	$\sigma = 180\rho_n - 286$	0.986
		$E = 179\rho_n - 285$	0.996
		$G = 72\rho_n - 113$	0.997

σ in MN m^{-2}, E in GN m^{-2}, G in GN m^{-2} and ρ_n in Mg m^{-3}.
*Data for "hgd" compacts only (green density 1.60 Mg m^{-3}) from [12].

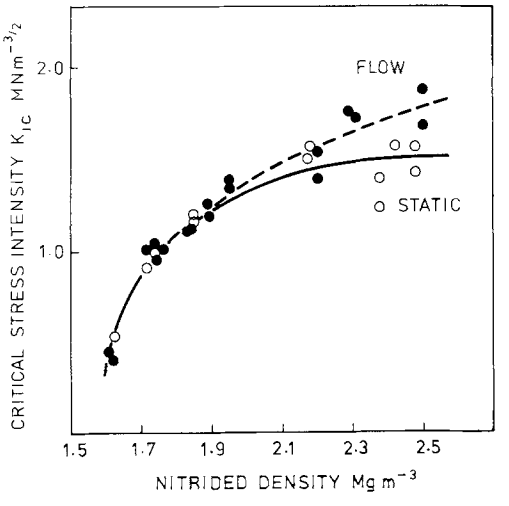

Figure 4 Critical stress intensity factor versus nitrided density for silicon compacts nitrided in "static" and "flowing" 95 N_2/5 H_2, series (a). [—o—o— "static" data, —●—●— "flow data].

are significantly different from the nitrogen "flow" data [12].

Linear relationships were also observed between E, G, σ and weight gain for series (a) experiments. Additionally the "best fit" extrapolated value for E at the theoretical density of silicon nitride (3.2 Mg m^{-3}) is 304 GN m^{-2}, similar to the value of 310 GN m^{-2} we have measured for fully dense hot-pressed silicon nitride containing 5% MgO densifying additive.

3.2. Fracture mechanics data for series (a)

The "faired-in" curve for ν (Fig. 2) was used to calculate the K_{IC} data shown in Fig. 4. In the present work 75 mm long double torsion plates were used and none of the K_{IC} data had to be rejected since the pre-crack lengths were always sufficiently remote from the end of each specimen to ensure that the first load to extend the pre-crack resulted in reliable K_{IC} data [12]. Small differences exist between "static" and "flow" K_{IC} data at high nitrided densities. The trends in these data are similar to those observed for samples reacted in nitrogen alone ("hgd" data of [12] supplemented by the additional data of Table III) although for densities > 1.9 Mg m^{-3} the values of K_{IC} are lower for samples reacted in 95 N_2/5H_2 (see Fig. 5). The critical surface defect sizes of length $2a$ were calculated from [12] as

$$2a = \frac{\pi K_{IC}^2(1-\nu^2)}{4\sigma^2}$$

using "best fit" data, and the variation with nitrided density for compacts reacted in "static" and "flowing" 95 N_2/5 H_2 is shown in Fig. 6 together with the corresponding data for compacts reacted in nitrogen ([12] and Table III). The critical defect

TABLE III Mechanical property data for 1.60 Mg m^{-3} green density silicon compacts reacted in "static" nitrogen (supplementing "hgd" "static" data from [12]).

Experiment		Strength bars			Modulus bars			K_{IC} plates	
Time (h)	Temperature (°C)	Weight gain (%)	Density (Mg m^{-3})	Mean strength (MN m^{-2})	E (GN m^{-2})	G (GN m^{-2})	Density (Mg m^{-3})	K_{IC} (MN m$^{-3/2}$)	Density Mg m^{-3})
0*	1100	0.5	1.61	17	–	–	–	–	–
0*	1170	5.7	1.70	38	33	14.7	1.69	0.92	1.72
0*	1200	11.7	1.80	70	55	23.0	1.80	–	–

*Furnace-cooled immediately reaction temperature achieved.

size decreases with increasing density for both "static" and "flow" materials. Notably $2a$ for "flow" materials is considerably reduced at all densities for 95 N_2/5 H_2 compared to nitrogen alone with values of about 50 μm and 105 μm respectively at a density of 2.58 Mg m^{-3}. At this density the differences between $2a$ for a 95 N_2/5 H_2 "static" material (35 μm) and a nitrogen "static" material (60 μm) or a 95 N_2/5 H_2 "flow" material (50 μm) are thought to be significant.

3.3. Isothermal reaction rates

Isothermal reaction rate data for compacts reacted in nitrogen and 95 N_2/5 H_2 at 1200° C are shown in Fig. 7. These data [15] serve to illustrate the very much higher reaction rates observed in 95 N_2/5 H_2. Enhanced reaction rates have been noted for other hydrogen concentrations in the range 1% to 10% [10]. Even in flowing 95 N_2/5 H_2 reaction rates are considerably greater than in static nitrogen.

3.4. Phase composition

Only α- and β-silicon nitride and silicon were detected as crystalline phases in samples from series (a) and (b) experiments. Significant amounts of non-crystalline phases must be absent since the oxygen contents of samples reacted to completion in 95 N_2/5 H_2 were typically less than 0.5 wt% and similar to those observed for samples reacted in nitrogen alone [8]. The variation of α- and β-contents with X-ray weight gain [9] for series (a) materials is shown in Fig. 8, together with the phase data for identical compacts reacted in "static" or "flowing" nitrogen (powder A′ in [9]). It is noted, as in [9], that predominantly α- forms at the early stages of the reaction with an increase in the relative proportion of β- as the extent of the reaction increases: the extent of the reaction and hence the relative α- or β-contents are however not necessarily related directly to temperature [9].

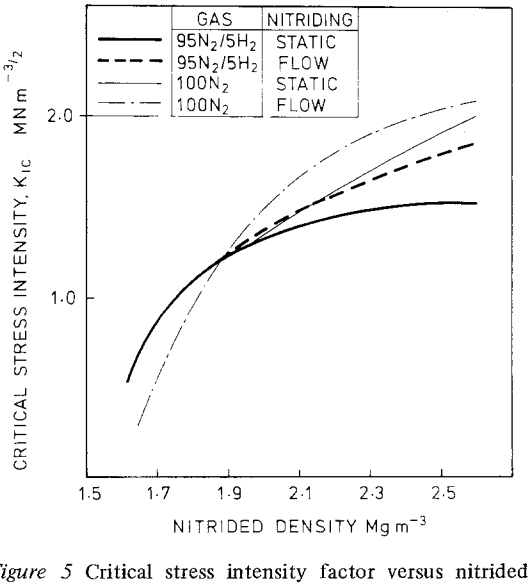

Figure 5 Critical stress intensity factor versus nitrided density for silicon compacts reacted in "static" and "flowing" 95 N_2/5H_2 [Series (a)] and "static" and "flowing" N_2 ("hgd" data from [12] and Table III).

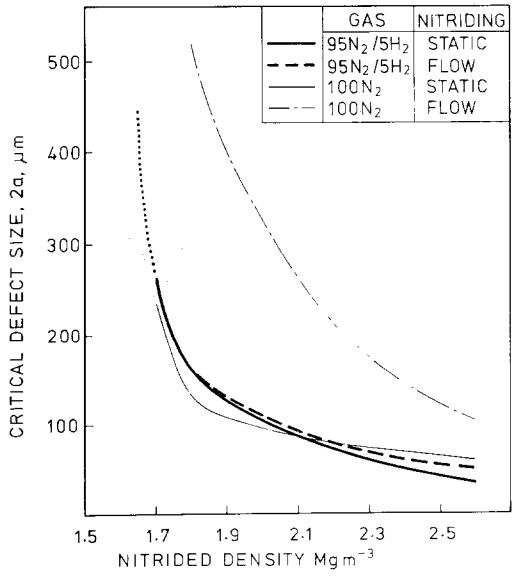

Figure 6 Critical defect size versus nitrided density for silicon compacts reacted in "static" and "flowing" 95 N_2/5H_2 [series (a)] and "static" and "flowing" N_2 ("hgd" data from [12] and Table III).

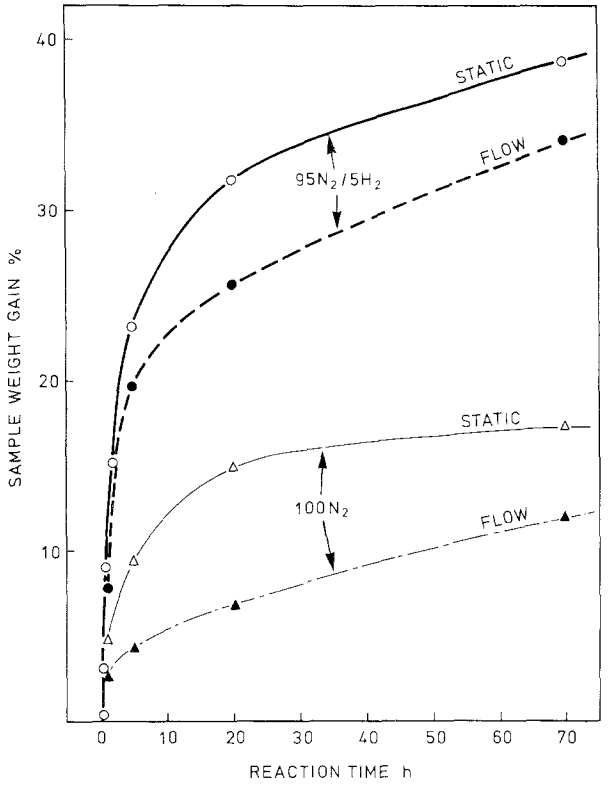

Figure 7 Isothermal reaction rate data for 1.60 Mg m^{-3} green density silicon compacts reacted in "static" or "flowing" N_2 and 95 N_2/5 H_2 at 1200° C.

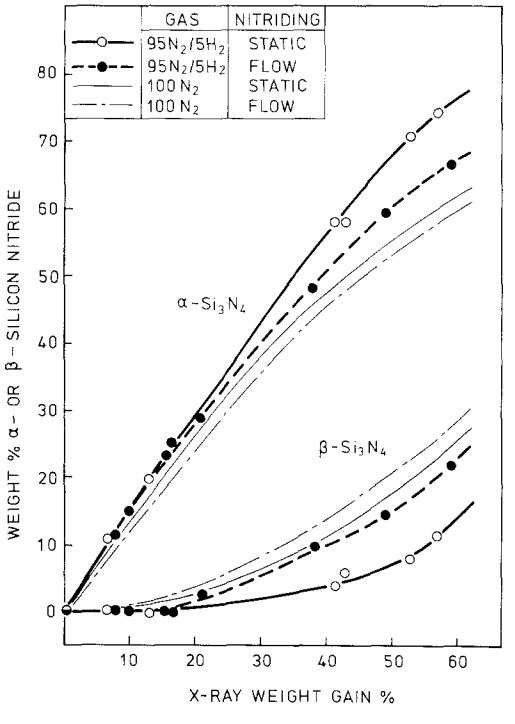

Figure 8 Composition as a function of X-ray weight gain for 1.60 Mg m^{-3} green density silicon compacts reacted in "static" or "flowing" N_2 [9] and 95 N_2/5H_2 [series (a)]. (Flow rate 100 ml min^{-1}.)

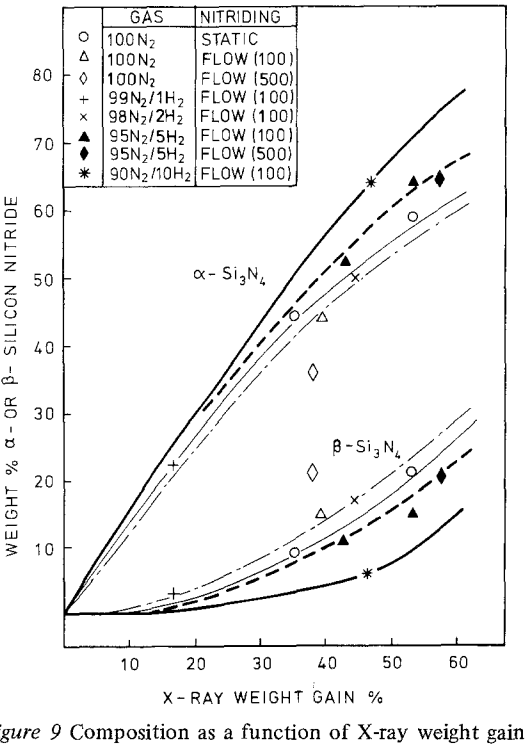

Figure 9 Composition as a function of X-ray weight gain for 1.60 Mg m^{-3} green density silicon compacts reacted in "flowing" N_2 containing various hydrogen concentrations, and in "static" N_2. Curves from Fig. 8. (Flow rates 100 or 500 ml min^{-1}.)

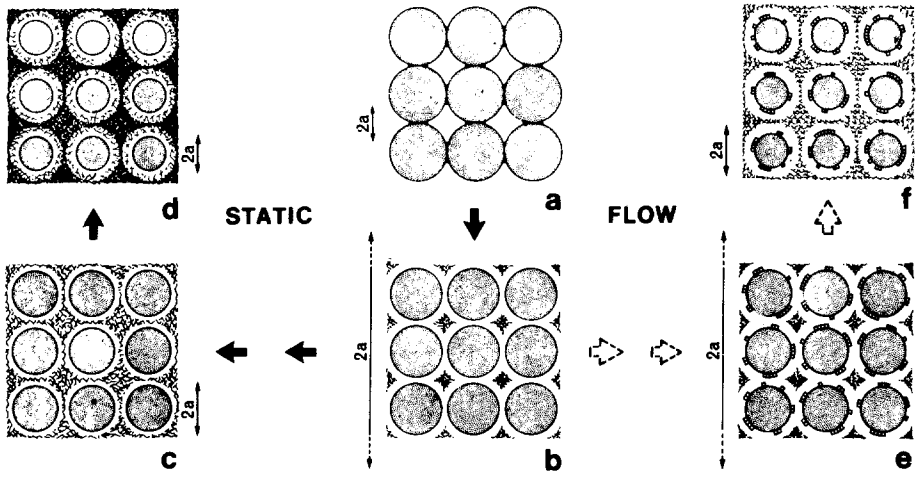

Figure 10 Schematic model for the nitridation of silicon compacts: (a) Green compact – silicon particles bonded by silicon or silica necks; (b) Early stages, static or flow (conversion < 5%) – necks destroyed, nitride network not continuous; (c) Static (~ 18% conversion) – nitride network continuous; (d) Static (~ 35% conversion) – nitride network thickening; (e) Flow (~ 18% conversion) – nitride layer on particles, network not continuous; (f) Flow (~ 35% conversion) – continuous nitride network established.

Higher α- contents are obtained at all densities with "static" or "flowing" $95\,N_2/5\,H_2$ than with either "static" or "flowing" nitrogen.

The variation of α- and β- contents with X-ray weight gain for differing nitrogen/hydrogen ratios [series (b)] and differing flow rates is shown in Fig. 9 together with the curves of Fig. 8 for comparison. There are consistent trends in these data. As the hydrogen content of the nitriding gas increases so the α- content increases. Increasing the flow rate from $100\,ml\,min^{-1}$ to $500\,ml\,min^{-1}$ considerably reduces the α- content and increases the β- content for nitrogen but has little effect for a $95\,N_2/5\,H_2$ composition.

3.5. Fractographic examination

Despite careful examination of the tensile edges of the fracture faces, fracture origins and "mirrors" could not be identified in strength tested bars. This together with the high linear correlation between strength and nitrided density suggests that in these experiments strength is controlled by the largest surface breaking pore (Section 2 and [12]). Typical fracture microstructures of these silicon compacts reacted to about 20% conversion to Si_3N_4 in $95\,N_2/5\,H_2$ and N_2 are shown in Figs. 13 and 14. The texture of the nitride network became finer as the reaction conditions were altered from "flowing" N_2, to "static" N_2, to "flowing" $95\,N_2/5\,H_2$, to "static" $95\,N_2/5\,H_2$. This trend corresponded to the trend in increasing reaction rates (Fig. 7) and increasing α-Si_3N_4 contents (Fig. 8).

4. Discussion

4.1. Structural and compositional models

Recently we have postulated models describing the development of the phase composition [8, 9] and structure [12, 13] of reaction-sintered silicon nitride. The compositional model suggests that α-Si_3N_4 probably forms from reactions involving silicon monoxide and nitrogen (silicon monoxide acting as the transport medium for silicon to the reaction site) whereas β-Si_3N_4 probably results from reactions between nitrogen and "clean" (unoxidized) silicon surfaces, silicon vapour or liquid silicon depending on the experimental conditions. The structural model [12, 13] suggests that under "static" nitriding conditions the necks between silicon particles are gradually eliminated during the early stages of nitridation and subsequently a continuous skeletal silicon nitride network develops within the pore space of the original compact (see Fig. 10). Thus the critical defects change from voids between silicon particles in the green compact to voids (containing the reacting silicon spheres) in the developing silicon nitride network. In "flowing" nitrogen the partial pressure of silicon monoxide (p_{SiO}) within the compact is probably reduced because SiO is lost from the compact and increased β-silicon nitride contents are recorded. The lower strengths and elastic

moduli and larger critical defect sizes which result are thought to be the consequence of a greater proportion of silicon nitride forming on the surface of silicon particles where it does not contribute as effectively to the continuous silicon nitride network [12, 13].

Reaction mechanisms and nitriding conditions that increase the "effective" partial pressure of silicon monoxide and also *allow* its reaction with nitrogen within the pore space of the compact in general should encourage network formation, and this will be reflected by high strengths and in general high α-silicon nitride contents (there are exceptions under conditions of low reaction rate [16]). Similarly nitriding conditions that favour the local removal of silicon monoxide from within the compact, (at a constant nitrogen partial pressure) such as the use of high flow rates with pure nitrogen and/or the use of oxygen getters adjacent to the sample should discourage the formation of network silicon nitride. This in turn should hinder the attainment of high strength, and promote the formation of a greater proportion of β-Si_3N_4 through a direct silicon/nitrogen surface reaction.

4.2. Reassessment of linear strength/nitrided density relationships

Our structural model [12, 13] was derived from data for high green density "hgd" ($1.60\,Mg\,m^{-3}$) and low green density "lgd" ($1.47\,Mg\,m^{-3}$) silicon compacts prepared from the same powder nitrided under "static" conditions. A linear strength/nitrided density relationship was established for the density range 1.54 to $2.50\,Mg\,m^{-3}$ that was independent of green density. A separate linear strength/density relationship was observed for compacts reacted in "flowing" nitrogen. "Static" strengths were always significantly higher than "flow" strengths. The lowest measured nitrided densities were $1.63\,Mg\,m^{-3}$ "lgd" or $1.78\,Mg\,m^{-3}$ "hgd" for "static" experiments and $1.54\,Mg\,m^{-3}$ "lgd" or $1.68\,Mg\,m^{-3}$ "hgd" for "flow" experiments. It was noted [12] that whilst the linear "flow" data extrapolated to approximately the green strength of the particular "hgd" compact (~10 $MN\,m^{-2}$ at $1.60\,Mg\,m^{-3}$) the "static" data extrapolated to a much higher strength (~50 $MN\,m^{-2}$ at $1.60\,Mg\,m^{-3}$). Similar but less definite trends were observed for "lgd" data. Thus under "static" conditions the strength must increase rapidly after the initial destruction of the silicon or silica necks (Fig. 10). This rapid strengthening in the early stages of nitridation prior to the establishment of a continuous network and the resultant linear relationships between strength and nitrided density accounts for the strength differences between "static" and "flow" materials at any particular nitrided density once the continuous network has been established.

We have now acquired additional data (Table III) for the "hgd" silicon compacts of [12] reacted in "static" nitrogen in the density range 1.60 to $1.80\,Mg\,m^{-3}$ (0 to ~18% conversion to Si_3N_4) and these are shown in Fig. 11 together with the "hgd" data of [12] and the strength data of this paper. For "hgd" compacts reacted in "static" nitrogen and "static" or "flow" 95 $N_2/5H_2$ strength increases rapidly at the early stages of nitridation before the respective linear portions of the strength/density relationships are established. Strengths are not significantly different for these three groups of nitriding conditions. For "hgd" compacts reacted in "flowing" nitrogen the strength/density relationship appears to remain linear for *all* densities. This offers a first explanation for the significant strength differences at constant density of "hgd" compacts reacted in "static" nitrogen, or "static" or "flowing"

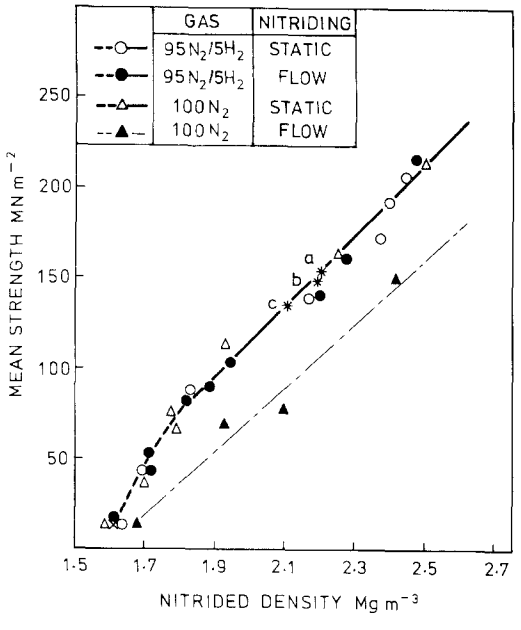

Figure 11 Strength versus nitrided density for $1.60\,Mg\,m^{-3}$ green density silicon compacts reacted in "static" or "flowing" N_2 ("hgd" data [12] and Table III) and 95 N_2/5 H_2 [series (a)]. (X – silicon compact; *– "flowing" N_2 plus water vapour).

95 N_2/5 H_2 compared with compacts reacted in "flowing" nitrogen (Figs. 3, 11 and [7, 10]). This suggests that the presence of hydrogen strongly favours the rapid formation of an initial skeletal silicon nitride network even under "flow" conditions.

Thus for silicon compacts reacted in "static" nitrogen and "static" or "flowing" 95 N_2/5 H_2 the linear strength/density and modulus/density relationships apply once the continuous network has been established. For our compacts of green density 1.60 Mg m^{-3} this seems to occur (Figs. 3, 11) at a density of about 1.80 Mg m^{-3}. Therefore it is important to identify the degree of conversion from silicon to silicon nitride necessary before linearity is established between strength and density and the relationship can be considered to be truly independent of green density. The degree of conversion will depend on both the nitriding conditions and the green density; the lower the green density, the more open the structure, the larger the pores in the silicon compact, and the higher the degree of conversion required before the continuous network is established [12]. Identical experimental observations and arguments apply to the development of Young's modulus and its independence of green density (see Fig. 12).

Additionally we have found that as for strength [12, 13], Young's and rigidity moduli of the silicon compacts are invariably larger than the values for the same compacts after minimal nitridation (conversion to silicon nitride of less than 1%). In terms of our structural model these reductions in modulus correspond to the initial destruction of the silicon interparticle necks in the green compact.

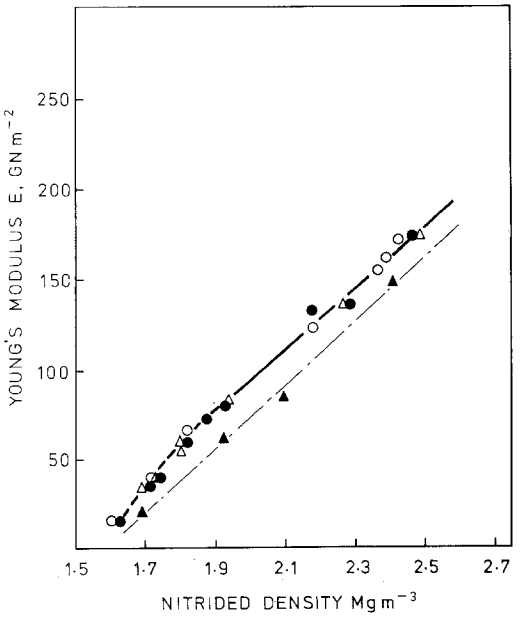

Figure 12 Young's modulus versus nitrided density for 1.60 Mg m^{-3} green density silicon compacts reacted in "static" or "flowing" N_2 or 95 N_2/5 H_2. Data and symbols as in Fig. 11.

For completeness we should reconsider the strength/density relationship at high conversion levels to silicon nitride. In [14] and [17] we discuss an "apparent" reduction in strength at high nitrogen weight gains with values lower than those anticipated from the strength/nitrided density relationships. However most of these lower than anticipated strengths at high conversions are probably related to other strength/density lines pertinent to the particular conditions existing during the fabrication of the samples [18]: were data available at that time for the low and intermediate levels of conversion this effect would have been apparent. The existence of undetected nitrogen gas flow [7], or batch to batch variations in silicon median particle size and size distribution [9] both result in an altered strength/density relationship: for gas flow this would be reflected by "apparent" reductions in strength when considering data for fully converted compacts only. There are however circumstances where the "apparent" strength reductions from values anticipated from strength/density relationships represent a real effect. Particular examples we have observed are when silicon particles melt during part of the nitriding cycle due to the selection of an incorrect nitriding temperature in relation to the reaction rate of the compact [19], or where large solid impurities become strength controlling [20].

4.3. Silicon nitride formation in the presence of hydrogen

For high purity nitrogen (oxygen content $p_{O_2} \sim 10^{-6}$ bar) silicon monoxide is generated by the reaction

$$Si(s) + SiO_2(s) \rightleftharpoons 2SiO(g) \qquad (1)$$

where p_{SiO} for this reaction can be 2×10^{-3} bar at 1327° C. Silicon monoxide is transported into the network/porosity to form α-Si_3N_4

$$3SiO(g) + 2N_2(g) \rightleftharpoons Si_3N_4(s) + \tfrac{3}{2}\, O_2(g) \qquad (2)$$

Although ΔG for Equation 2 is positive when all components are in their standard state, oxygen

is removed by reaction with either solid silicon or silicon vapour to form silica, thus lowering p_{O_2}. Depending on the oxygen partial pressure in relation to the SiO partial pressure this oxidation will be either active or passive, and if active the silica will be regenerated as silicon monoxide according to Equation 1, enabling Reaction 2 to continue. When p_{O_2} exceeds the partial pressure of silicon monoxide from Equation 1 (2×10^{-3} bar at 1327° C), passivating silica layers should be formed, although experimentally we have shown that oxygen pressures in the bulk gas up to 10^{-1} and 2×10^{-2} bar can be tolerated in "static" and "flowing" nitrogen respectively [8] with the formation of only α- and β-silicon nitride phases.

Silicon monoxide therefore will be continuously generated as long as silicon and oxygen remain. The relative concentration of p_{SiO} within the compact will determine the amount of α-Si_3N_4 formed whereas the β-Si_3N_4 content will be determined by the relative contribution of nitrogen reacting with clean silicon surfaces, or silicon vapour (vapour pressure $\sim 1 \times 10^{-7}$ bar at 1327° C [21]).

Hydrogen can be expected to modify the course of these reactions in the following ways. Hydrogen will react with silica according to

$$SiO_2(s) + H_2(g) \rightleftharpoons SiO(g) + H_2O(g) \quad (3)$$

and depending on the water vapour concentration the partial pressure of silicon monoxide from Reaction 3 could be similar to p_{SiO} from Reaction 1, i.e. $\sim 10^{-3}$ bar at 1327° C. Increases in the SiO signal have been observed by mass spectrographic methods when silicon with a surface oxide layer has been heated in nitrogen/hydrogen mixtures as compared to pure nitrogen [22].

Residual water vapour in the furnace tube and water vapour generated from side reactions (for example Reaction 3) may react with silicon according to

$$Si(s, g) + H_2O(g) \rightleftharpoons SiO(g) + H_2(g) \quad (4)$$

or

$$Si(s, g) + 2H_2O(g) \rightleftharpoons SiO_2(s) + 2H_2(g) \quad (5)$$

depending on the partial pressure of silicon monoxide and hydrogen within the system. Thus a series of cyclic reactions may occur: the extent of any one reaction and its relative contribution within the compact will be determined predominantly by the surface silica content of the silicon compact, the oxygen and water vapour levels in the furance (either as residuals, impurities entrained in the gas supply or evolved from the furnace tube), the nitridation temperature, the added hydrogen concentration and the rate of removal of vapour species from the region of the reacting compact (for example by getters or in a flowing gas stream). The presence of hydrogen is believed to favour Reaction 3, and increases in the partial pressure of silicon monoxide should result at all nitridation temperatures.

The possible formation of silicon hydrides and their subsequent reaction with nitrogen are unlikely to be significant processes. The maximum partial pressures p_{SiH} or p_{SiH_4} (for example) at 1327° C are about 10^{-9} bar, lower than the corresponding vapour pressure of silicon (10^{-7} bar) and considerably lower than the partial pressures of silicon monoxide (about 10^{-3} bar).

4.4. Phase compositions for nitridation in the presence of hydrogen

We have suggested above that hydrogen increases the partial pressure of silicon monoxide and the compositional model suggests that this increases the amount of α-Si_3N_4 formed. For series (a) experiments it is quite clear from Fig. 8 that the addition of 5% hydrogen to "static" or "flowing" nitrogen increases the α-Si_3N_4 content at all X-ray weight gains. That the α-Si_3N_4 contents are higher with "static" than "flowing" $95\,N_2/5\,H_2$ may be a consequence of the concentrating effect of hydrogen within the furnace in "static" conditions resulting in increases in the effective p_{H_2} and p_{SiO} levels. Therefore it is not immediately clear whether there is significant loss of SiO from the compact in a $95\,N_2/5H_2$ nitriding gas flow: the enhanced reaction rates observed in nitrogen/hydrogen gases ([10] and Fig. 7) may minimize considerably any SiO losses.

The systematic increase in α-Si_3N_4 content with increasing hydrogen content (and increasing p_{SiO}) at constant flow rate can be seen in Fig. 9 where the curves are the data from Fig. 8. Increasing the flow rate from $100\,ml\,min^{-1}$ to $500\,ml\,min^{-1}$ for a $95\,N_2/5\,H_2$ gas composition has little effect on the α-Si_3N_4 content, possibly because reaction rates of SiO with N_2 when there are hydrogen additions are accelerated. Thus the local partial pressure of silicon monoxide is not greatly influenced by the higher flow rate. For pure nitrogen (Fig. 9) the increased flow rate

markedly reduces the α-Si_3N_4 content because the nitrogen gas flow removes silicon monoxide, reaction rates are slower [7, 15] and the partial pressure of silicon monoxide is reduced.

Further support for these mechanisms is given by consideration of the β-Si_3N_4 contents (Figs. 8 and 9) which are determined independently of the α-Si_3N_4 contents [8]. The β-Si_3N_4 contents are reduced as the hydrogen concentration increases, suggesting a reduction of the direct β-Si_3N_4 forming silicon–nitrogen reaction. As the nitrogen flow rate increases, the amount of β-Si_3N_4 increases, suggesting an increase in the amount of the direct silicon–nitrogen reaction.

4.5. Mechanical properties – nitridation in the presence of hydrogen

We have suggested earlier in this paper that reactions which encourage network formation should favour high strength, whereas the loss of network-forming vapour-transported species should result in larger defects and lower strengths. Additionally we have suggested that in flowing $95\,N_2/5\,H_2$, hydrogen increases the silicon monoxide partial pressure and the reaction rate, particularly at the early stages of nitriding, and thereby minimizes the loss of vapour-transported species and favours the rapid formation of the skeletal silicon nitride network. The experimental

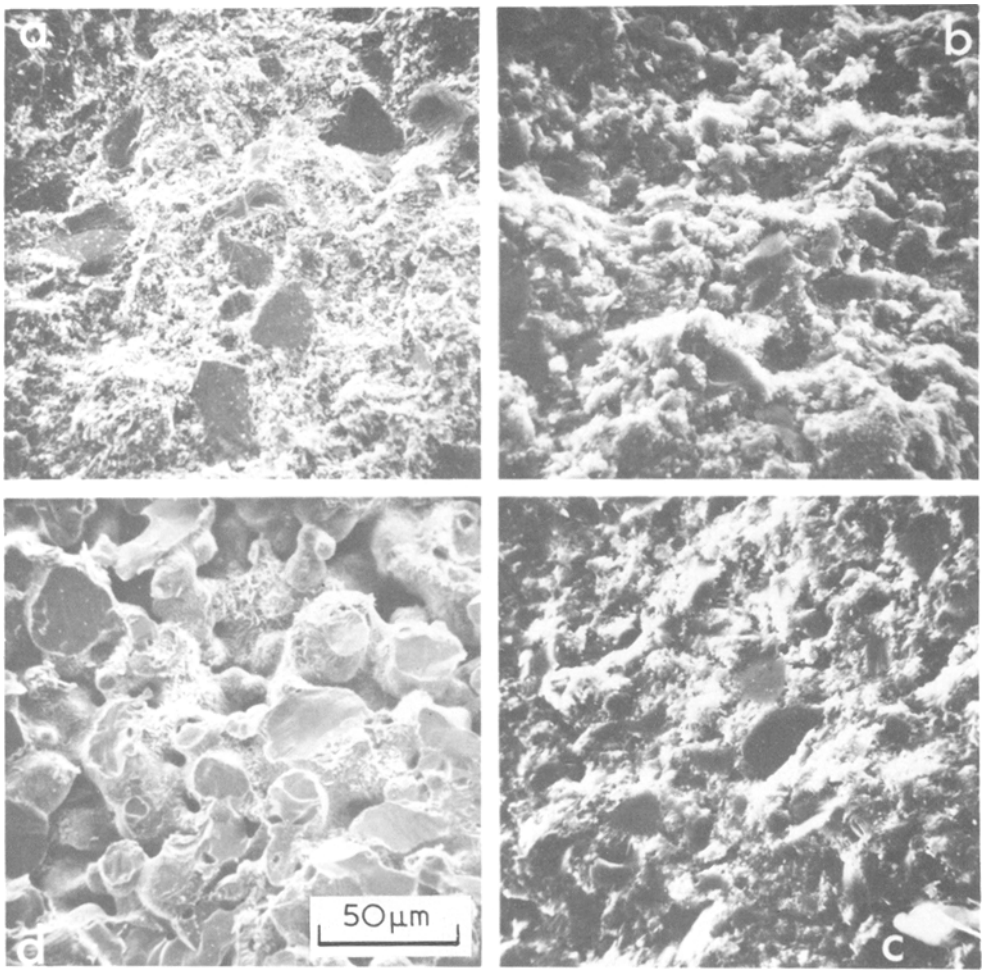

Figure 13 Typical scanning electron micrographs of fracture surfaces of $1.60\,Mg\,m^{-3}$ silicon compacts reacted in differing nitriding environments (conversions all about 20%). (a) "Flowing" N_2, (b) "static" N_2, (c) "flowing" $95\,N_2/5\,H_2$, (d) very pure gettered "flowing" N_2. [The microstructures of compacts reacted in "static" $95\,N_2/5\,H_2$ are similar to those shown in (c)].

data recorded support these arguments. Microstructural examination of compacts reacted in "static" or "flowing" $95\,N_2/5\,H_2$ showed a lack of surface nitride layers and a fine structure of the nitride network (Figs. 13c and 14c). Additionally the reduction in critical defect size (Fig. 6) and higher E values observed for samples reacted in "flowing" $95\ N_2/5H_2$ compared to "flowing" nitrogen both imply a reduction in the proportion of "redundant" silicon nitride [12] which in turn would explain their higher strengths.

The similarity in shape of the σ/ρ_n and E/ρ_n curves at low silicon to silicon nitride conversions (1.6 to $1.9\,Mg\,m^{-3}$) for "static" N_2 and "static" and "flowing" $95\,N_2/5\,H_2$ (Figs. 11 and 12) is probably a result of the existence of a minimum effective SiO pressure which aids network formation and eliminates the formation of surface layers and loss of SiO from the compact (cf. N_2 flow). The near identical slopes of the σ/ρ_n curves for the groups of nitriding conditions considered here (and the E/ρ_n curves) for densities $> 1.8\,Mg\,m^{-3}$ (conversions $> 18\%$) suggest that at higher densities the network (irrespective of the proportion of α- or β-Si_3N_4) develops in such a way that $\Delta\sigma/\Delta\rho_n$ is the same for all the nitriding conditions considered in this paper (including flowing N_2). This similarity in slope probably occurs because $\rho_n > 1.8\,Mg\,m^{-3}$ corresponds to the higher nitriding temperatures where higher p_{SiO} levels occur and reaction rates are increased so that the influence of gas flow is a diminishing effect. Recently acquired strength data for isothermal nitriding at 1150 and 1300° C have shown this supposition to be correct: large strength differences were observed between "static" and "flow" materials reacted in nitrogen at 1150° C but the strength differences were negligible for isothermal nitriding at 1300° C [15].

Modulus/density and strength/density lines of lower slope than observed for "static" nitriding would be expected under circumstances where gas flow has a significant effect and reduces p_{SiO} over *all* levels of conversion. Such a situation might arise either with very high gas flow rates, or with flowing pure nitrogen and coarse silicon powders where p_{SiO} concentrations per unit mass of sample and reaction rates are low (for example powder C of [7]).

Thus changes in the composition of the nitriding atmosphere have a significant influence on microstructure and mechanical properties, and property changes can be interpreted in terms of our compositional [8, 9] and structural models [12, 13].

4.6. Further confirmation of structural and compositional models

4.6.1. Increased vapour phase contribution to network formation

The addition of hydrogen with the resultant increase in p_{SiO} particularly at the early stages of the reaction has been shown to be one mechanism that increases network formation and eliminates the adverse effect on strength observed with samples reacted in flowing nitrogen. Increased p_{SiO} levels in flowing nitrogen should also be obtained by adding water vapour to the nitriding gas (for example Equations 4 and 5). Strength data for silicon compacts (identical to those used in series (a) and (b) experiments) reacted in flowing nitrogen ($100\,ml\,min^{-1}$ flow rate) containing water vapour at concentrations of 7×10^{-3}, 1×10^{-2} and 2×10^{-2} bar are shown in Fig. 11 as points a, b and c respectively. These data confirm that water vapour has a similar effect to hydrogen on network formation when added to flowing nitrogen.

4.6.2. Decreased vapour phase contribution to network formation

We have suggested in Section 4.1 and [12, 13] that reaction mechanisms favouring surface layer formation and/or the loss of vapour species from the reacting compact will discourage network formation and the ultimate attainment of high strength. Such processes will occur with reactions containing very low levels of oxygen (and hence the restricted potential to form silicon monoxide), and/or where there are high gas flow rates and/or low reaction rates [7]. We have reacted $1.60\,Mg\,m^{-3}$ compacts prepared from the same relatively impure batch of silicon powder used for series (a) and (b) experiments in highly purified flowing nitrogen (flow rate $200\,ml\,min^{-1}$) at reaction temperatures up to 1330° C. The samples were heated under vacuum for 2 h at 1330° C to remove surface silica layers prior to the admission of

TABLE IV Phase composition of $1.60\,Mg\,m^{-3}$ green density silicon compacts reacted in very pure flowing nitrogen at 1330° C

Nitriding time (h)	X-ray weight gain (%)	Composition (wt%)		
		Si	α-Si_3N_4	β-Si_3N_4
5	10.7	84	10	6
100	21.3	68	23	9

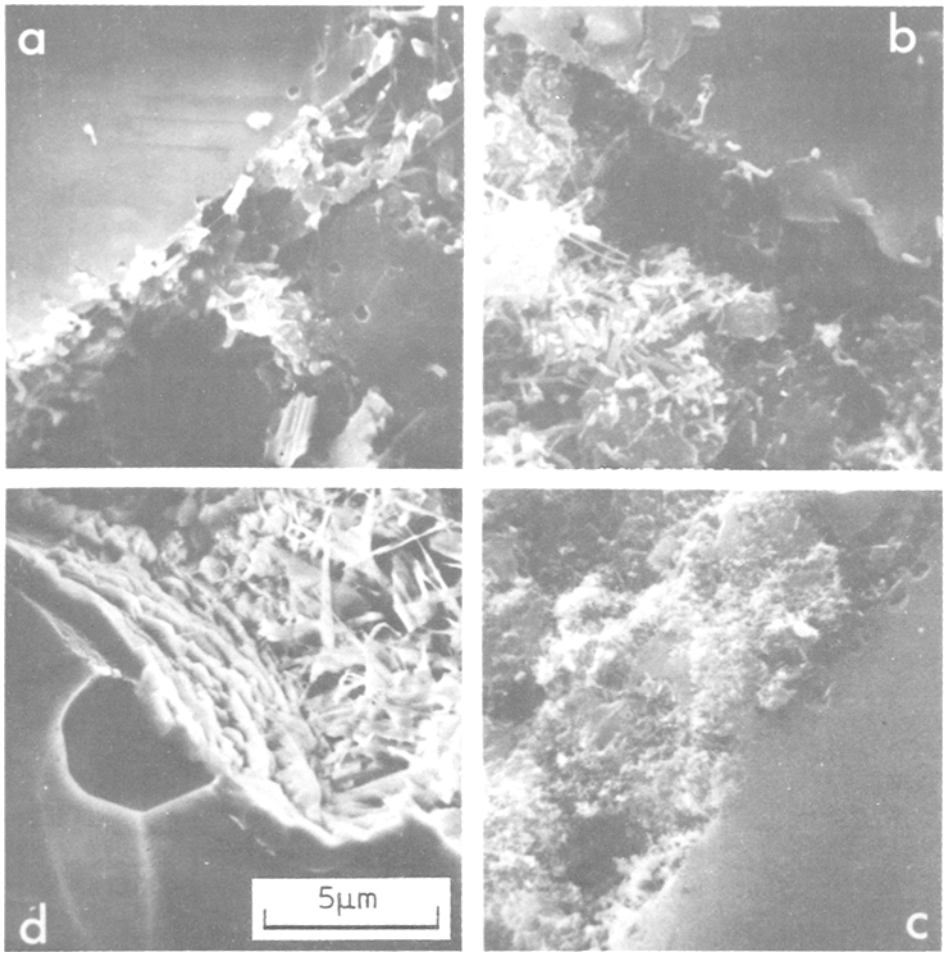

Figure 14 Typical scanning electron micrographs of fracture surfaces of 1.60 Mg m^{-3} silicon compacts reacted in differing nitriding environments (conversions all about 20%). (a) "flowing" N_2, (b) "static" N_2, (c) "flowing" $95\,N_2/5\,H_2$, (d) very pure gettered "flowing" N_2. Note the surface nitride layers in (d), and the increasing fineness of the nitride network (a) → (b) → (c) corresponding to an increase in reaction rate and p_{SiO} (see Fig. 15).

nitrogen and were surrounded by zirconium foil to act as an oxygen getter.

The phase data for these samples are shown in Table IV together with the observed and X-ray weight gains. X-ray weight gains greater than 20% could not be achieved and examination of the microstructure showed (Figs. 13d and 14d) that a complete silicon nitride surface layer had formed, blocking access to underlying silicon and stopping the reaction. The texture of this nitride layer was relatively coarse although there is some evidence of very limited vapour transport and stubby whisker formation (Figs. 13d and 14d). Table IV shows the much higher than normal β-silicon nitride contents. That this is so at low weight gains is important. The very low oxygen and silicon monoxide partial pressures within the compact resulting from the use of a very pure system, gettering, and flowing nitrogen have resulted in increased layer formation by reaction of nitrogen at "clean" silicon surfaces and increased β-Si_3N_4 contents. Silicon nitride surface layers of this morphology have been observed by Atkinson and co-workers [23]: the growth mechanisms in both cases may be similar although the silicon used in our work is relatively impure [12]. Part of the surface layers shown in Figs. 13d and 14d however, are almost certainly low aspect ratio α-Si_3N_4 (see

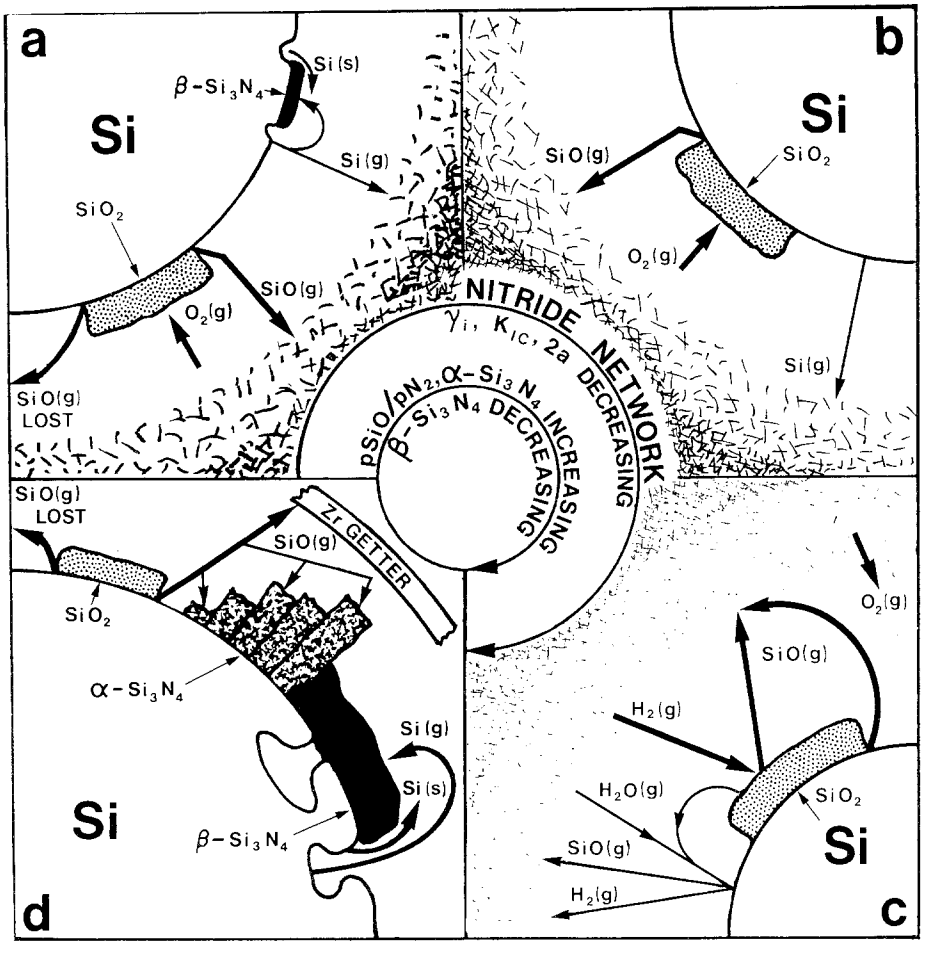

Figure 15 A schematic representation of the influence of the nitriding environment on the mechanism of formation of microstructure, composition and fracture properties of reaction-sintered Si_3N_4. (a, b, c, d as for Fig. 14). Only the principal reactions involved are shown: those in "heavy line" are considered to be important in determining microstructure and mechanical properties.

Table IV), grown under the very low silicon monoxide concentrations that probably still exist in the experimental system. Coherent α-silicon nitride surface layers have been observed by Guthrie [24] under these conditions on silicon single crystal slices. Whilst some loss of reactivity may have resulted from the vacuum heat-treatment due to silicon–silicon neck growth and a reduced internal surface area (but without an overall change in density), it is thought that the high purity gettered nitriding environment round the samples has controlled the formation of surface layers of silicon nitride. We have found that such vacuum pre-heated silicon compacts can be nitrided to near completion in ungettered static nitriding systems and extensive surface layers are not observed.

The inability to fully nitride such compacts in very pure nitrogen, therefore, makes it difficult to compare their strengths with the more usual silicon nitrides where strength is controlled by network development. For the limited nitrided density range achieved, compacts with extensive surface layers were weaker than compacts with nitride networks.

5. Formation and properties of reaction-sintered silicon nitride

A summary of the influence of the nitriding environment on the mechanism of formation of microstructure, composition and fracture properties of reaction-sintered silicon nitride is shown in Fig. 15. The four "case histories", "flowing" N_2 (a), "static" N_2 (b), "flowing" 95 N_2/5 H_2 (c) and very pure gettered "flowing" N_2 (d), have been chosen as representing four well-defined and reported nitriding conditions. This figure also

shows a representation of the microstructural features including network texture that are observed fractographically (Figs. 13 and 14). It is difficult to show clearly in one figure all possible reactions occurring and Fig. 15 summarizes only the principal ones: those in heavy line are considered to be important in determining microstructure, and hence mechanical properties, and phase composition. Fig. 15 demonstrates that the nitriding environment has a most important control over the properties and composition of reaction-sintered silicon nitride and that for a given silicon compact it is the direct participation of silicon monoxide as the principal transport medium for silicon to form a silicon nitride network within the pore space of the original silicon compact [12] that is of prime importance for the development of high strength.

From the published literature it is clear that nitridation environments vary from laboratory to laboratory, however it is thought that the ideas presented in this paper together with the references to earlier work (for example [6–14]) should enable reaction mechanisms and changes in material processing to be assessed and interpreted and should provide a basic framework to aid development of reaction-sintered silicon nitride with improved engineering properties.

6. Conclusions

(1) The nitriding environment has an important control over the properties and compositions of reaction-sintered silicon nitride.

(2) The addition of hydrogen to a "static" or "flowing" nitriding gas during the formation of reaction-sintered silicon nitride has the following results:

(a) "flowing" and "static" strength/density and modulus/density relationships are coincident with those for "static" nitrogen;

(b) the deleterious effect of gas flow on strength and modulus in nitrogen is eliminated;

(c) critical defect sizes at any particular density are similar to those observed in "static" nitrogen but considerably smaller than for "flowing nitrogen;

(d) at any particular density the α-Si_3N_4 content is increased by an amount dependent upon the hydrogen concentration;

(e) isothermal reaction rates are increased;

(f) the microstructure of the silicon nitride network is finer.

(3) The addition of water vapour to a nitriding gas also eliminates the deleterious effect of gas flow on strength and modulus.

(4) In very pure flowing nitrogen (low oxygen levels) complete reaction of the silicon particles is inhibited by the formation of surface layers of silicon nitride.

(5) These observations can be explained, in conjunction with our structural and compositional models, in terms of the rôle of silicon monoxide and its reactions to form α-silicon nitride in the nitride network.

(a) Hydrogen or water vapour enable a high partial pressure of silicon monoxide to be maintained at the early stages of nitridation even in the presence of gas flow. Enhanced reaction rates in the presence of hydrogen ensure the rapid establishment of a "skeletal" network of predominantly α-silicon nitride which aids the development of mechanical properties.

(b) When the partial pressure of silicon monoxide is low the formation of β-silicon nitride on silicon particles becomes more favoured. This leads to the development of silicon nitride surface layers which impede nitridation and which will not contribute effectively to the skeletal silicon nitride network.

Acknowledgements

The authors are indebted to B. J. Luxton, W. May and J. Studley for experimental assistance, Mrs. J. Irvine for scanning electron microscopy and to W. R. Davis (British Ceramic Research Association) for modulus measurements. This article is published by permission of the Controller HMSO, holder of Crown Copyright.

References

1. N. L. PARR, G. F. MARTIN and E. R. W. MAY, "Special Ceramics", edited by P. Popper (Haywood and Co., London 1960) p. 102.
2. A. F. McLEAN, Proceedings of the 2nd Army Materials Technology Conference on Ceramics for High Performance Applications, edited by J. J. Burke, A. E. Gorum and R. N. Katz (Brook Hill, Chestnut Hill, Mass, 1974) p. 9.
3. R. J. BRATTON and A. N. HOLDEN, *ibid.* (1974) p. 37.
4. D. J. GODFREY, Ceramics for High Performance Applications Conference, Newport, RI, USA (1977) to be published.
5. D. J. GODFREY and M. W. LINDLEY, *Proc. Brit. Ceram. Soc.* **22** (1973) 229.
6. B. F. JONES and M. W. LINDLEY, *Powder Met. Int.* 8 (1976) 32.

7. *Idem, J. Mater. Sci.* **11** (1976) 1288.
8. D. P. ELIAS and M. W. LINDLEY, *J. Mater. Sci.* **11** (1976) 1278.
9. D. P. ELIAS, B. F. JONES and M. W. LINDLEY, *Powder Met. Int.* 8 (1976) 162.
10. B. F. JONES and M. W. LINDLEY, *J. Mater. Sci.* **11** (1976) 1969.
11. J. A. MANGELS, *J. Amer. Ceram. Soc.* 58 (1975) 354.
12. B. F. JONES, K. C. PITMAN and M. W. LINDLEY, *J. Mater. Sci.* **12** (1977) 563.
13. *Idem,* "Nitrogen Ceramics", edited by F. L. Riley (Noordhoff, Leyden, 1977) p. 561.
14. B. F. JONES and M. W. LINDLEY, *J. Mater. Sci.* **10** (1975) 967.
15. B. LUXTON and M. W. LINDLEY, Admiralty Marine Technology Establishment (Holton Heath) data - to be published.
16. M. W. LINDLEY, K. C. PITMAN and B. F. JONES, "Fracture Mechanics of Ceramics", Vol. 4, edited by R. C. Bradt, D. P. H. Hasselman and F. F. Lange (Plenum Press, New York, 1978) p. 921.
17. B. F. JONES and M. W. LINDLEY, Proceedings of the 8th International Conference on Science of Ceramics (The British Ceramic Society, Stoke-on-Trent, 1976) p. 123.
18. *Idem, J. Mater. Sci.* **11** (1976) 191.
19. *Idem,* Admiralty Marine Technology Establishment (Holton Heath) Unpublished data.
20. *Idem,* as for [13] p. 577.
21. P. GRIEVESON and C. B. ALCOCK; "Special Ceramics", edited by P. Popper (British Ceramic Research Association, Stoke-on-Trent, 1960) p. 183.
22. S. S. LIN, *J. Amer. Ceram. Soc.* 58 (1975) 271.
23. A. ATKINSON, A. J. MOULSON and E. W. ROBERTS, *J. Amer. Ceram. Soc.* 59 (1976) 285.
24. R. B. GUTHRIE and F. L. RILEY, *Proc. Brit. Ceram. Soc.* **22** (1973) 275.

Received 30 December 1977 and accepted 1 June 1978.